

MR Imaging in Male Infertility¹

Rosaleen B. Parsons, MD

Andrea M. Fisher, MD

Natan Bar-Chama, MD

Harold A. Mitty, MD

In patients with male infertility, endorectal magnetic resonance (MR) imaging provides high-resolution images of the prostate gland and ejaculatory apparatus. The multiplanar capability of MR imaging allows production of a detailed map of the reproductive tract for guiding treatment. Causes of male infertility can be classified as congenital, acquired, infectious, or hormonal. Wolffian duct abnormalities include agenesis of the kidney, vas deferens, or seminal vesicle and cysts of the vas deferens, seminal vesicle, or urogenital sinus-ejaculatory duct. Müllerian duct abnormalities are less common and consist of müllerian duct cysts and utricle cysts. Cowper duct cysts and peripheral-zone prostatic cysts are acquired causes of male infertility. Prostatitis, an infectious cause of male infertility, may mimic carcinoma on long repetition time/echo time images. A low testosterone level is one of the hormonal causes of male infertility. Pitfalls in the interpretation of MR images can be avoided by familiarity with normal and abnormal findings in patients with male infertility.

■ INTRODUCTION

Fifteen percent of couples in the United States are infertile (1). Difficulty in conceiving is usually attributable to female sterility; however, a male factor can be found in close to half of the cases (1). When a male factor is clinically suspected, imaging of the ejaculatory apparatus is performed. Vasography can be performed with ultrasound (US) or fluoroscopic guidance and requires cannulation of the vas deferens (deferent duct) and injection of contrast material to opacify the ejaculatory apparatus (Fig 1). Although vasography is the traditional method of evaluating the male genital tract, it is invasive and carries a risk of postprocedure stricture of the vas deferens (2).

Transrectal US and computed tomography (CT) are the most commonly used noninvasive techniques for investigating the male reproductive tract. However, US is operator dependent and may not accurately depict a dilated, tortuous genital tract. CT involves radiation and lacks multiplanar capability. A third noninvasive technique, endorectal magnetic resonance (MR) imaging, has multiplanar capability and provides high-resolution images of the prostate gland and adjacent structures.

Abbreviation: SE = spin echo

Index terms: Genitourinary system, abnormalities, 84.147 • Genitourinary system, MR, 84.12149 • Sterility

RadioGraphics 1997; 17:627-637

¹ From the Departments of Radiology (R.B.P., A.M.F., H.A.M.) and Urology (N.B.C.), Mount Sinai Medical Center, One Gustave L. Levy Pl, New York, NY 10029. Presented as a scientific exhibit at the 1995 RSNA scientific assembly. Received July 15, 1996; revision requested September 5 and received December 26; accepted December 31. **Address reprint requests to R.B.P.**

© RSNA, 1997

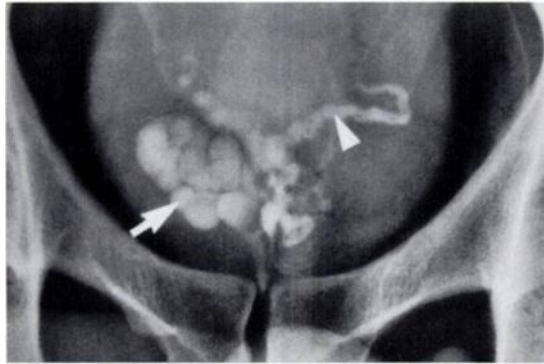


Figure 1. Vasogram obtained to confirm patency of the vasa deferentia (arrowhead) shows an opacified right seminal vesicle (arrow). The left seminal vesicle was not evaluated.

Knowledge of the normal and abnormal appearances of the male reproductive tract on MR images can help one avoid diagnostic pitfalls. In this article, we present the MR imaging features of lesions associated with male infertility. Such lesions include congenital (wolffian and müllerian duct anomalies), acquired (Cowper duct and peripheral-zone prostatic cysts), infectious (prostatitis), and hormonal (seminal vesicle atrophy) entities.

■ TECHNIQUE OF MR IMAGING

Our patients are imaged with a 1.5-T MR unit (Signa; GE Medical Systems, Milwaukee, Wis). A disposable endorectal coil is placed in the rectum and insufflated, and 1 mg of glucagon is administered intramuscularly. After obtaining a sagittal T1-weighted localizer image with a phased-array coil, 4-mm-thick contiguous sections are acquired in the axial, sagittal, and coronal planes. The following parameters are used: 500/12 (repetition time msec/echo time msec) for T1-weighted images and 4,000/150 for fast spin-echo (SE) images (Fig 2).

■ EMBRYOLOGIC DEVELOPMENT

A basic knowledge of the development of the genitourinary tract is helpful in understanding the anatomic and pathologic features of male infertility (Fig 3) (Table 1).

Three paired excretory organs appear sequentially in the fetus: the pronephros, mesonephros, and metanephros. The pronephros forms in the 3rd fetal week and consists of tubules that join the bilateral pronephric ducts. The ducts enter the cloaca and evolve into the wolffian ducts.

Table 1
Embryologic Origins of the Male Genital Tract

Embryologic Structure	Permanent Structures
Mesonephric tubules	Efferent ductules of epididymis
Wolffian duct	Renal collecting system, ureter, vas deferens, seminal vesicle, ejaculatory duct, epididymis, appendix of epididymis
Müllerian duct*	Appendix of testis, prostatic utricle
Urogenital sinus	Urinary bladder, prostate gland, prostatic utricle

*Also called the paramesonephric duct.

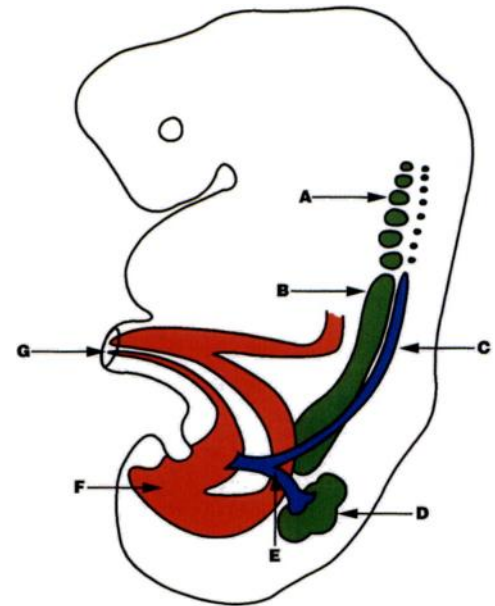


Figure 3. Drawing (lateral view) shows a 5-week-old embryo. A = pronephros, B = mesonephros, C = wolffian (mesonephric) duct, D = metanephros, E = ureteric bud, F = cloaca, G = allantois. (Adapted and reprinted, with permission, from reference 3.)

The mesonephros, a temporary, functioning, primitive kidney, appears as the pronephros degenerates. The ureteric buds (metanephric ducts) branch from the wolffian ducts at 5 fetal weeks. These buds detach from the wolffian ducts, extend caudally, and meet the metanephric blastemas. Each bud eventually be-

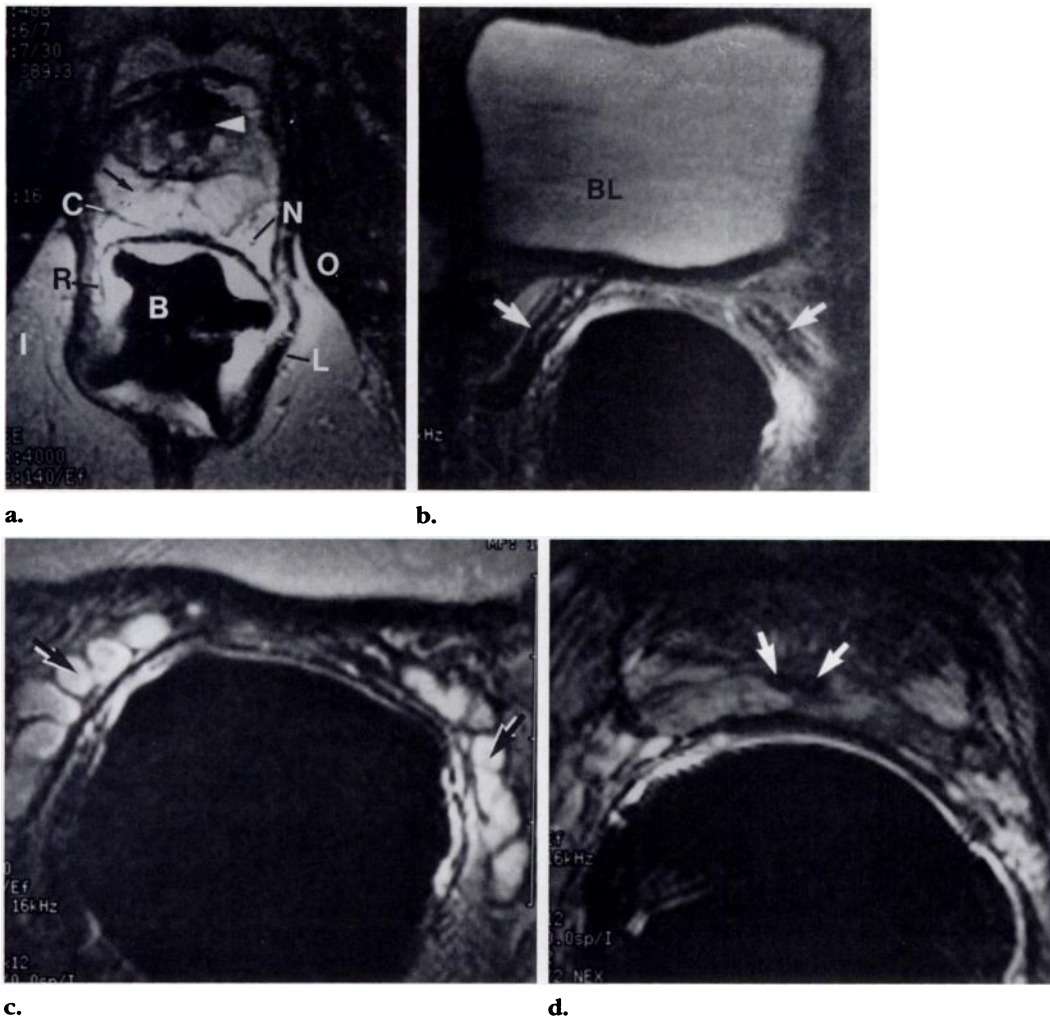


Figure 2. (a) Axial fast SE MR image (4,000/140) shows the central prostate gland (arrowhead) and peripheral zone (arrow). *B* = rectal balloon, *C* = prostatic capsule, *I* = ischiorectal fossa, *L* = levator ani muscle, *N* = neurovascular bundle, *O* = obturator internus muscle, *R* = rectal wall. (b) Axial fast SE MR image (5,500/147) shows the vasa deferentia (arrows). *BL* = urinary bladder. (c) Axial fast SE MR image (5,500/147) shows the seminal vesicles (arrows). (d) Axial fast SE MR image (5,500/147) shows the ejaculatory ducts (arrows).

comes a ureter and collecting system, while the blastemas form the metanephros or permanent kidney.

The wolffian duct persists and matures into the male internal genital tract: the appendix of the epididymis, paradidymis, epididymis, vas deferens, ejaculatory duct, seminal vesicle, and hemitrigone of the bladder.

The müllerian ducts are induced by the wolffian ducts at 5 fetal weeks. The müllerian ducts grow caudally, join in the midline, and fuse with an outgrowth of the urogenital sinus.

This region becomes the prostatic utricle, which has no known function. The müllerian ducts involute secondary to müllerian regression factor, which is secreted by the Sertoli cells of the testis. The appendix of the testis is a müllerian duct remnant.

The urogenital sinus arises from the cloaca and develops into the bladder and urethra. The prostate gland derives from the urethra (3-6).

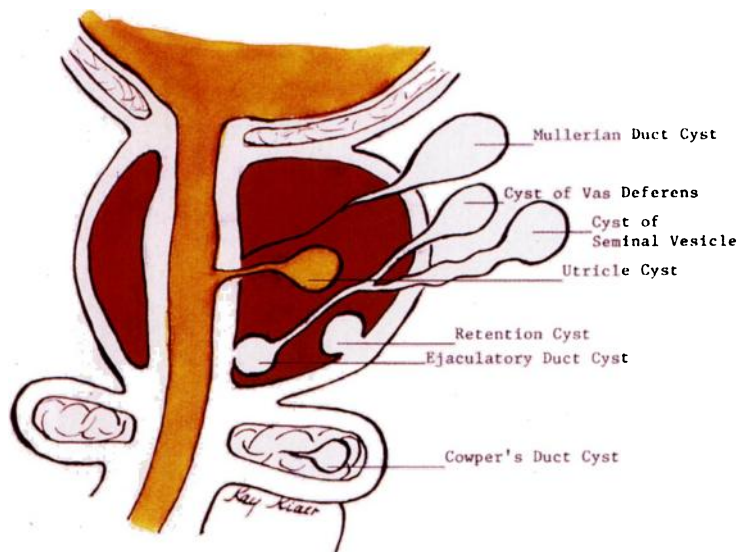


Figure 4. Drawing shows prostatic and periprostatic cysts. (Adapted and reprinted, with permission, from reference 8.)

■ CAUSES OF MALE INFERTILITY

Numerous abnormalities can be seen with endorectal MR imaging. They can be classified as congenital, acquired, infectious, or hormonal (Table 2). In our experience, congenital abnormalities predominate. Developmental errors that occur early in gestation (before 7 weeks) are often severe and involve the wolffian and müllerian ducts and ureteric bud. Defects occurring after 8 weeks usually cause isolated wolffian or müllerian duct abnormalities (7). These abnormalities may manifest as prostatic cysts (Fig 4).

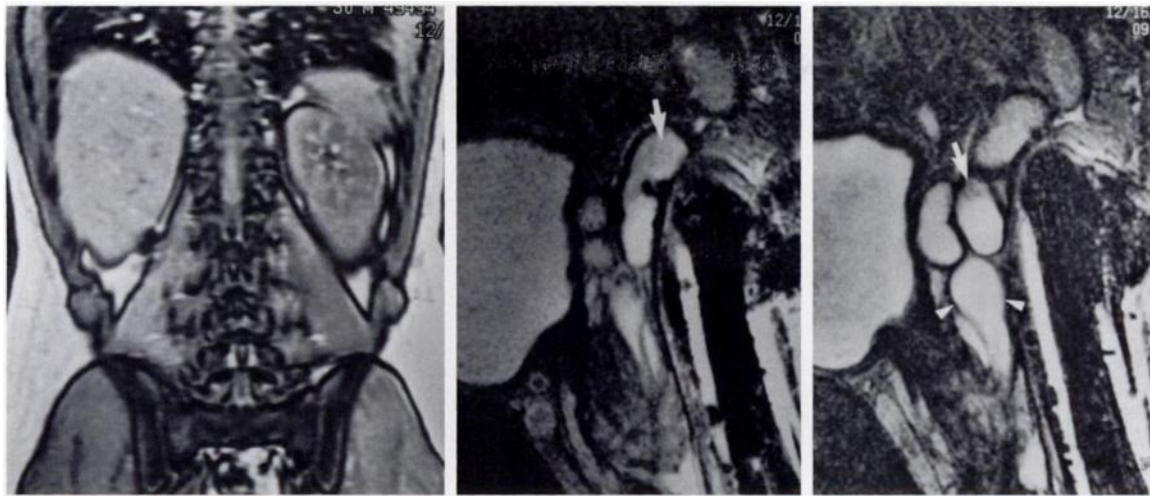
● Congenital Lesions

Wolffian Duct Anomalies.—Wolffian duct abnormalities are more common than müllerian duct abnormalities and include renal agenesis, agenesis of the vas deferens, absent or small seminal vesicles, and seminal vesicle cysts (6). Less common anomalies include ejaculatory duct cysts and urogenital sinus-ejaculatory duct cysts.

Table 2
Causes of Male Infertility

Congenital	
Wolffian duct anomalies	
Renal agenesis or atrophy	
Vas deferens agenesis or cyst	
Seminal vesicle agenesis or cyst	
Ejaculatory duct cyst	
Müllerian duct anomalies	
Müllerian duct cyst	
Utricle cyst	
Acquired	
Cowper duct cyst	
Peripheral-zone prostatic cyst	
Infectious	
Prostatitis	
Hormonal	
Seminal vesicle atrophy	

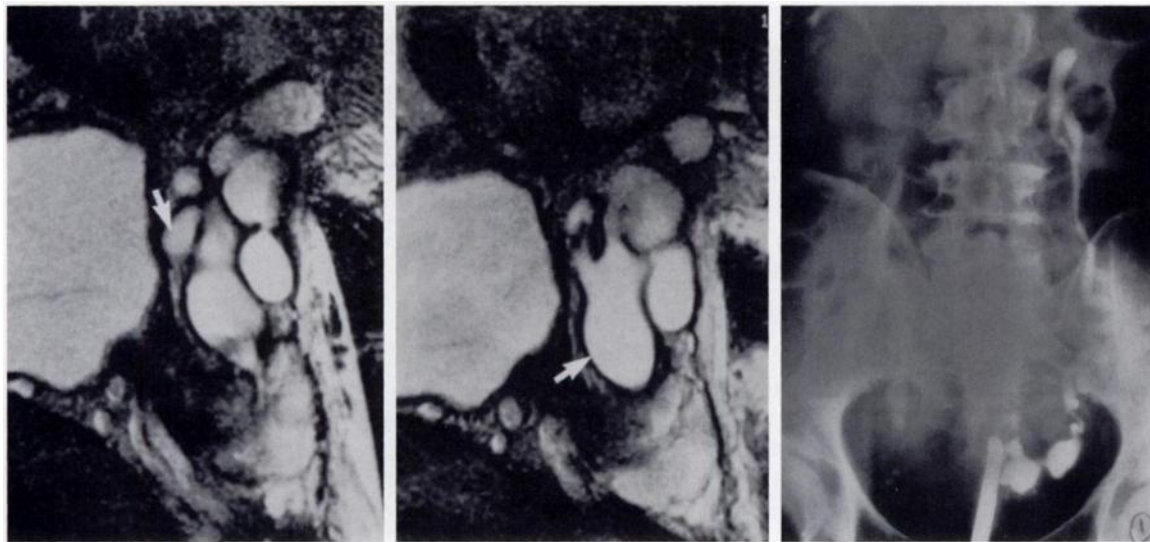
Zinner syndrome is renal agenesis or dysgenesis with ipsilateral seminal vesicle cysts (9,10). Unilateral renal agenesis is seen in about 0.1% of the population (5). It occurs when the ureteric bud fails to meet the metanephric blastema and induce the development of the kidney. There is a high association with ipsilateral genital tract anomalies, the most common of which are seminal vesicle abnormalities (Fig 5).



a.

b.

c.



d.

e.

f.

Figure 5. Zinner syndrome. (a) Coronal MR image obtained with a fast multiplanar spoiled gradient-echo sequence (100/13.8) shows absence of the right kidney. (b) Sagittal fast SE MR image (4,000/147) shows an ectopic, blind-ending ureter (arrow). (c) Sagittal fast SE MR image (4,000/147) slightly lateral to b shows the ureter (arrow) entering a dilated seminal vesicle (arrowheads). (d) Sagittal fast SE MR image (4,000/147) shows a dilated vas deferens (arrow). (e) Sagittal fast SE MR image (4,000/147) shows a dilated seminal vesicle. (f) Retrograde urethrogram of another patient with similar examination results shows left renal agenesis and a blind-ending, bifid ureter with ectopic insertion into a seminal vesicle cyst.

Figures 6, 7. (6) Axial fast SE MR image (4,000/147) shows congenital absence of the vasa deferentia. The linear structures of high signal intensity anterior to the prostate gland are vascular and mimic the vasa. The normal vasa are convoluted, not linear. (7) Coronal fast SE MR image (3,000/130) shows congenital absence of the left seminal vesicle and vas deferens. There is a seminal vesicle cyst in an atrophic right seminal vesicle (arrow). Arrowhead indicates where the vas deferens should enter the prostate gland.



6.



7.

Unilateral agenesis of the vas deferens is present in 1%–7% of otherwise normal males (11). Bilateral agenesis is present in about 1% of infertile men and is associated with cystic fibrosis (12) (Fig 6). Almost all patients with unilateral or bilateral agenesis have seminal vesicle abnormalities (11).

Hypoplastic, atrophic, or absent (Fig 7) seminal vesicles may be a cause of infertility. Hypoplastic seminal vesicles are defined as smaller than 11 mm but greater than 7 mm in width. Atrophic seminal vesicles are defined as smaller than 7 mm in width (13). The semen is low in volume, lacks fructose, and has an acid pH. The spermatozoa are absent or dysmotile (14,15).

Urogenital sinus–ejaculatory duct cysts are rare midline prostatic cysts derived from the wolffian duct and urogenital sinus. Because both ejaculatory ducts enter these cysts, the cysts may contain spermatozoa. These cysts can be extremely large and extend beyond the prostate gland (8,16,17) (Fig 8).

Müllerian Duct Anomalies.—Müllerian duct cysts and utricle cysts are separate entities (18,19). The müllerian duct cyst is derived from

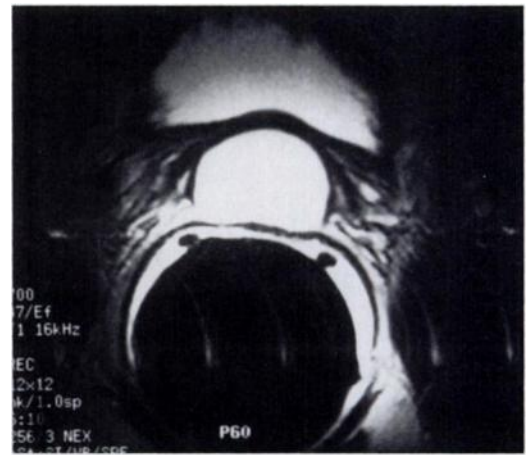
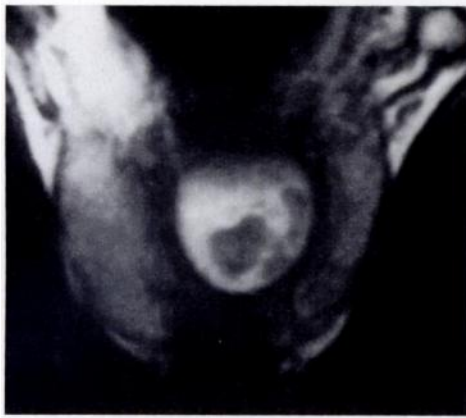


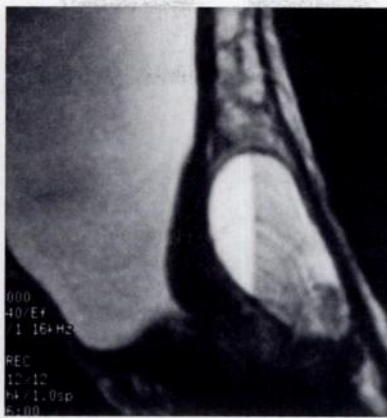
Figure 8. Axial fast SE MR image (7,700/147) shows a large, midline, hemorrhagic ejaculatory duct cyst.

the müllerian duct, whereas the utricle cyst derives from a dilatation of the prostatic utricle. Radiographically, these entities can be identical and indistinguishable from urogenital sinus–ejaculatory duct cysts. Large müllerian duct and utricle cysts may cause obstruction.

Müllerian duct cysts occur in 4%–5% of male newborns and in 1% of men (20). Usually, the cysts are discovered in infertile men in the 3rd



9a.



9b.



10a.



10b.

Figures 9, 10.

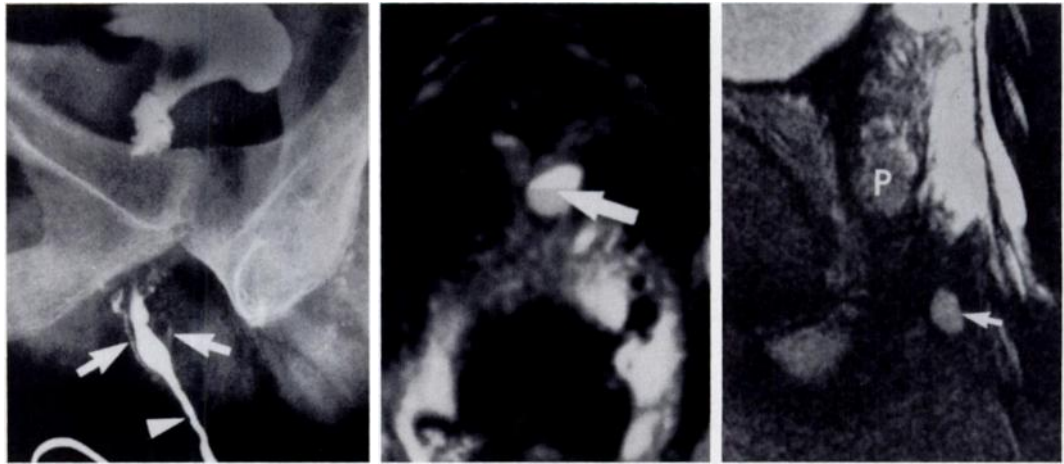
(9a) Coronal fast SE MR image (3,000/126) shows a hemorrhagic and debris-filled müllerian duct cyst. (9b) Sagittal fast SE MR image (5,000/126) shows the hematocrit effect of blood within the cyst. (10) Axial (5,000/140) (a) and coronal (3,000/130) (b) fast SE MR images show a utricle cyst.

or 4th decade of life; such cysts are the most common cause of ejaculatory duct obstruction in this subgroup (2,21). Associated genital tract anomalies are rare.

The cysts are spherical and intraprostatic and do not communicate with the prostatic urethra. When large, they extend superolaterally above the prostate gland and may contain hemorrhage and debris (16) (Fig 9). It is debatable whether müllerian duct cysts can contain spermatozoa (21,22). Most researchers believe that these cysts do not communicate with the genital tract. Both müllerian duct cysts and utricle

cysts are associated with an increased rate of prostatic carcinoma (23,24).

Utricle cysts manifest in the first 2 decades of life and are often associated with hypospadias, intersex disorders, cryptorchidism, or ipsilateral renal agenesis (8). Unlike müllerian duct cysts, utricle cysts do not extend beyond the prostate gland. They communicate freely with the prostatic urethra and contain spermatozoa (Fig 10).



11. **12a.** **12b.**
Figures 11, 12. (11) Retrograde urethrogram shows an anterior urethral stricture (arrowhead) and retrograde filling of the Cowper glands (arrows). (12a) Axial fast SE MR image (4,000/147) shows blood within a Cowper duct cyst (arrow). (12b) Sagittal fast SE MR image (4,000/147) shows a Cowper duct cyst (arrow). P = prostate gland.

● **Acquired Lesions**

The Cowper (bulbourethral) glands are paired accessory sexual organs analogous to the Bartholin glands in females. Just before ejaculation, the Cowper glands secrete a mucoid material that provides an alkaline milieu and lubricant for the spermatozoa. The main gland lies within the urogenital diaphragm. The duct drains into the bulbar urethra (25-27) (Fig 11).

Lesions of the Cowper glands are rare; in an autopsy study, the prevalence of such lesions was 2.3% (28). The ducts can become obstructed and form retention cysts. Several cases of prenatal and early postnatal death secondary to urinary obstruction from large retention cysts have been reported (29-34). In adults, Cowper duct cysts occur due to infection or trauma (26,28,35). Most such cysts are asymptomatic; however, large cysts may cause urinary symptoms including hematuria, bloody urethral discharge, and postvoiding dribbling. Sagittal and coronal images can be helpful in identifying the urogenital diaphragm origin of these cysts (Fig 12).

Acquired prostate cysts are smooth-walled, peripherally located cysts. They are categorized as parasitic cysts, cysts associated with carcinoma,

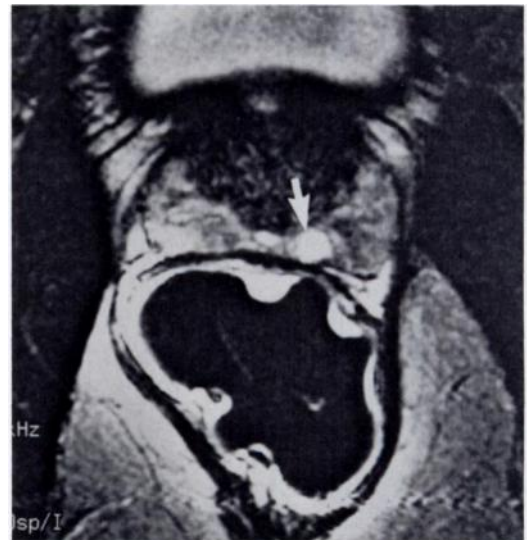


Figure 13. Axial fast SE MR image (4,000/147) shows an incidentally found prostatic retention cyst (arrow) in the left peripheral zone.

noma, and retention cysts (Fig 13). These cysts do not communicate with the genital tract or contain spermatozoa (8,36).

The pathogenesis of prostatic retention cysts is unknown; however, their frequency increases with age, and they are seen in patients with benign prostatic hypertrophy (37). Infer-



14.



15.

Figures 14, 15. (14) Coronal fast SE MR image (4,000/130) shows prostatitis. The peripheral gland demonstrates diffuse decreased signal intensity (arrow). (15) Axial fast SE MR image (5,500/147) shows tuberculous prostatitis. Diffuse, abnormal low signal intensity is present in the peripheral zone (arrow).

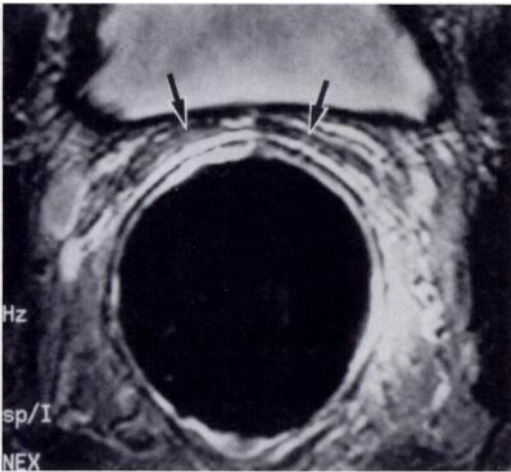


Figure 16. Axial fast SE MR image (4,000/138) shows atrophic seminal vesicles (arrows) secondary to a low testosterone level.

tile patients have been found to have a higher prevalence of retention cysts than fertile control patients (2).

● Infectious Lesions

Prostatitis is acute inflammation of the prostate gland. The causes of prostatitis are numerous; however, nonbacterial causes predominate (38). On long repetition time/echo time MR images, chronic prostatitis and granulomatous

prostatitis appear as low-signal-intensity abnormalities in the peripheral zone that are indistinguishable from the abnormalities of carcinoma (39,40) (Fig 14). Stenotic or atrophic seminal vesicles have been identified in cases of bacterial prostatitis, which can cause infertility (41).

Tuberculous prostatitis (Fig 15) is rare. The infection usually affects persons 20–40 years of age (42). Primary tuberculous prostatitis is uncommon; secondary infection develops after passage of infected urine through the prostatic urethra. Ejaculatory duct strictures can develop (21).

● Hormonal Lesions

The hormonal status of the patient plays a significant role in fertility. Luteinizing hormone, which is produced in the pituitary gland, is the major regulator of testosterone synthesis. Testosterone, which is produced by the Leydig cells, is required for spermatogenesis, prostate growth, and production of seminal vesicle secretions (43). A low testosterone level is one of the hormonal causes of male infertility (Fig 16). Low testosterone levels can be improved with clomiphene citrate (Clomid; Marion Merrell Dow, Kansas City, Mo), which induces production of luteinizing hormone.

■ CONCLUSIONS

MR imaging of the male genital tract will not replace transrectal US in the initial evaluation of patients with infertility. Endorectal MR imaging should be reserved for selected patients in whom results of transrectal US are not definitive. We and other investigators have found the multiplanar capability of MR imaging beneficial in identifying and tracing the paths of ectopic, tortuous ureters and in detecting and quantifying the extent of disease of the seminal vesicle, vas deferens, and prostate gland (44). MR images can serve as a "map" for guiding interventional diagnostic or corrective procedures.

Acknowledgments: We thank Gifty Mensah and Gail Aguilar for help in the preparation of the manuscript.

■ REFERENCES

1. Templeton A. Infertility: epidemiology, aetiology, and effective management. *Health Bull (Edinb)* 1995; 53:294-298.
2. Jarow JP. Transrectal ultrasonography of infertile men. *Fertil Steril* 1993; 60:1035-1039.
3. Moore KL. *The developing human: clinically oriented embryology*. 3rd ed. Philadelphia, Pa: Saunders, 1982.
4. Herman TE, McAlister WH. Radiographic manifestations of congenital anomalies of the lower urinary tract. *Radiol Clin North Am* 1991; 29:365-382.
5. Trigaux JP, Van-Beers B, Delchambre F. Male genital tract malformations associated with ipsilateral renal agenesis: sonographic findings. *JCU* 1991; 19:3-10.
6. McDermott V, Orr JD, Wild SR. Duplicated müllerian duct remnants associated with unilateral renal agenesis. *Abdom Imaging* 1993; 18: 193-195.
7. Hall S, Oates RD. Unilateral absence of the scrotal vas deferens associated with contralateral mesonephric duct anomalies resulting in infertility: laboratory, physical, and radiographic findings and therapeutic alternatives. *J Urol* 1993; 150:1161-1164.
8. Nghiem HT, Kellman GM, Sandberg SA, et al. Cystic lesions of the prostate. *RadioGraphics* 1990; 10:635-650.
9. Zinner A. Ein fall von intravesikaler Samenblasenzyste. *Wien Med Wochenschr* 1914; 64: 605.
10. King BF, Hattery RR, Lieber MM, et al. Congenital cystic disease of the seminal vesicle. *Radiology* 1991; 178:207-211.
11. Honig SC, Lamont J, Oates RD. Ultrasonographic renal and seminal vesicle anomalies in patients with bilateral congenital absence of the vas deferens (abstr). *J Urol* 1991; 145:326A.
12. Vazquez-Levin MH, Kupchik GS, Torress Y, et al. Cystic fibrosis and congenital agenesis of the vas deferens, antisperm antibodies, and CF-genotype. *J Reprod Immunol* 1994; 27:199-212.
13. Honig SC. Use of ultrasonography in the evaluation of the infertile man. *World J Urol* 1993; 11:102-110.
14. Menkveld R, Oettle TFK, Swanson RJ, Acosta A, Oehninger S. *Atlas of human sperm morphology*. Baltimore, Md: Williams & Wilkins, 1991.
15. Gilbert BR, Cooper GC, Goldstein M. Semen analysis in the evaluation of male factor subfertility. *AUA Update Series* 1992; 11:250-255.
16. Elder JS, Mostwin JL. Cyst of the ejaculatory duct/urogenital sinus. *J Urol* 1984; 132:768-771.
17. Brooks RT. Cyst of the ejaculatory duct: a case report. *J Urol* 1969; 101:881-883.

18. Van Poppel H, Vereecken R, DeGeeter P, et al. Hemospermia owing to utricular cyst: embryological summary and surgical review. *J Urol* 1983; 129:608-609.
19. Schwartz JM, Bosniak MA, Hulnick DH, et al. Computed tomography of midline cysts of the prostate. *J Comput Assist Tomogr* 1988; 12: 215-218.
20. Higashi TS, Takizawa K, Suzuki S, et al. Müllerian duct cyst: ultrasonographic and computed tomographic spectrum. *Urol Radiol* 1990; 12:39-44.
21. Pryor JP, Hendry WF. Ejaculatory duct obstruction in subfertile males: analysis of 87 patients. *Fertil Steril* 1991; 56:725-730.
22. Ng JW, Kong CK, Wong MK. Opening of both vasa into a müllerian duct cyst. *J Pediatr Surg* 1993; 28:756-757.
23. Francis RA, Lewis E. Ultrasonic demonstration of a müllerian duct cyst. *J Ultrasound Med* 1983; 2:525-526.
24. Szemes GC, Rubin DJ. Squamous cell carcinoma in a müllerian duct cyst. *J Urol* 1968; 100:40-43.
25. Cowper W. Two new glands near the prostate glands with their excretory ducts, lately discovered. *Philos Trans Coll Lond* 1699; 21: 364-369.
26. Currarino G, Fuqua R. Cowper's glands in the urethrogram. *AJR* 1972; 116:838-842.
27. Peter SM, Neil AN, Robert LL. Retention cysts of Cowper's duct. *Radiology* 1976; 120:377-380.
28. William AB, George WK. Lesions of Cowper's glands in children. *J Urol* 1979; 122:121-123.
29. Yaffe D, Zissin R. Cowper's glands duct: radiographic findings. *Urol Radiol* 1991; 13:123-125.
30. Johnson FP. Diverticula and cysts of the urethra. *J Urol* 1923; 10:295-302.
31. Howell C, Lisanski ET, Scott E. Congenital cysts of the urethra in a three-week-old male infant causing pyonephrosis and death. *Bull Sch Med Univ Md* 1942; 26:241-246.
32. Cook FE, Shaw JL. Cystic anomalies of the ducts of Cowper's glands. *J Urol* 1961; 85:659-664.
33. Weinberger MA. Urethral cysts arising in Cowper's glands ducts: Aetiology, pathogenesis, and clinico-pathological aspects. *J Urol* 1961; 85:818-826.
34. Abrams HJ, Joshi DP, Neier CR. Intrauterine urinary retention and electrolyte imbalance secondary to Cowper's glands cyst. *J Urol* 1966; 95:565-567.
35. Hodgson CJ, Edwards D. A textbook of x-ray diagnosis by British authors. 4th ed, vol 5. Philadelphia, Pa: Saunders, 1970; 507.
36. Gevenois PA, Van Sinoy ML, Sintzoff SA Jr, et al. Cysts of the prostate and seminal vesicles: MR imaging findings in 11 cases. *AJR* 1990; 155:1021-1024.
37. Hamper UM, Epstein JI, Sheth S, et al. Cystic lesions of the prostate gland: a sonographic-pathologic correlation. *J Ultrasound Med* 1990; 9:395-402.
38. Pfav A. Prostatitis: a continuing enigma. *Urol Clin North Am* 1986; 13:695-715.
39. Bryan DJ, Butler HE, Nelson AO, et al. Magnetic resonance imaging of the prostate. *AJR* 1986; 146:543-548.
40. Schiebler ML, Tomaszewski JE, Bezzi M, et al. Prostatic carcinoma and benign prostatic hyperplasia: correlation of high-resolution MR and histopathologic findings. *Radiology* 1989; 172:131-137.
41. Baert L, Leonard A, D'Hoedt M, Vandeursen R. Seminal vesiculography in chronic bacterial prostatitis. *J Urol* 1986; 136:844-845.
42. Smith DR. General urology. Los Altos, Calif: Lange, 1978; 10, 20-23, 189-191, 440.
43. Mawhinney M, Tarry W. Male accessory sex organs and androgen action. In: Lipshultz L, Howards S, eds. *Infertility in the male*. 2nd ed. St Louis, Mo: Mosby-Year Book, 1991; 124-154.
44. Schnall MD, Pollack HM, Van-Arsdalen K, et al. The seminal tract in patients with ejaculatory dysfunction: MR imaging with an endorectal surface coil. *AJR* 1992; 159:337-341.